Numerical Analysis of Acoustic Characteristics in Gas Turbine Combustor with Spatial Non-homogeneity

Chae Hoon Sohn*
Department of Aerospace Engineering, Chosun University, Gwangju 501-759, Korea
Han Chang Cho
Research Institute of Industrial Science and Technology, San 32 Hyoja-dong, Nam-gu, Pohang 790-600, Korea

Acoustic characteristics in an industrial gas-turbine combustor are numerically investigated by a linear acoustic analysis. Spatially non-homogeneous temperature field in the combustor is considered in the numerical calculation and the characteristics are analyzed in view of acoustic instability. Acoustic analyses are conducted in the combustors without and with acoustic resonator, which is one of the acoustic-damping devices or combustion stabilization devices. It has been reported that severe pressure fluctuation frequently occurs in the adopted combustor, and the measured signal of pressure oscillation is compared with the acoustic-pressure response from the numerical calculation. The numerical results are in good agreement with the measurement data. In this regard, the phenomenon of pressure fluctuation in the combustor could be caused by acoustic instability. From the numerical results for the combustor with present acoustic resonators installed, the acoustic effects of the resonators are analyzed in the viewpoints of both the frequency tuning and the damping capacity. It is found that the resonators with present specifications are not optimized and thus, the improved specification or design is required.

Key Words : Acoustic Characteristics, Acoustic Instability, Gas Turbine Combustor, Acoustic Resonators

1. Introduction

Pressure oscillation frequently occurs in various combustors and usually affects the combustor operation unfavorably. There are many causes for pressure oscillation in the combustor, e.g., mechanical vibration of the combustor, feed-system interactions, acoustic instability, and etc. Especially, when the combustion system is complex, it is difficult to identify the main cause of undesirable pressure oscillation. For example, pressure oscillation in industrial gas turbine has intrigued the system operator and the main cause of the phenomenon has been pursued by many researchers (Lefebvre, 1998).

One of the main causes is acoustic instability resulting from the sound-wave amplification in the combustor, and thereby it has long gained attention in the propulsion and power systems. Under acoustic instability, pressure oscillations are amplified through in-phase heat addition/extraction from combustion, leading to acoustic resonance at specific acoustic modes of the chamber (Harrje and Reardon, 1972; Zucrow and Hoffman, 1977). It may lead to intense pressure fluctuation as well as excessive heat transfer to the combustor wall such as in the solid

* Corresponding Author,
E-mail : chsohn@chosun.ac.kr
TEL : +82-62-230-7123; **FAX** : +82-62-230-7123
Department of Aerospace Engineering, Chosun University, Gwangju 501-759, Korea. (Manuscript **Received** January 9, 2004; **Revised** May 6, 2004)

and liquid propellant rocket engines, ramjets, turbojet thrust augmentors, utility boilers, and furnaces (McManus et al., 1993). To understand this phenomenon, there have been conducted various fundamental works (Harrje and Reardon, 1972 ; Culick and Yang, 1995 ; Sohn et al., 1996 ; Seo, 2003 ; Yang et al., 2003), but it is still being pursued.

In understanding the acoustic instability, combustion is of particular interest because it is a fundamental source of the thermal energy that can be fed to amplify and sustain the acoustic oscillations (Flefil et al., 1996 ; Sohn, 2002a). But, when the pressure oscillation in the chamber is diagnosed in view of acoustic instability so as to find the main cause, it can offer sufficient information to investigate only the acoustic characteristics without considering its coupling with heat release from combustion. This concept arises from the fact that acoustic instability shows the clear and well-established acoustic field in the chamber when it occurs. Thus, as the first step for diagnosis of pressure oscillation, the investigation of acoustic characteristics is useful and cost-effective.

In this study, from a standpoint of acoustic instability, acoustic characteristics in the combustor of industrial gas turbine encountering with undesirable pressure oscillation, are investigated intensively through the linear acoustic analysis adopted in the previous works (Wicker et al., 1995 ; Sohn, 2002b ; Sohn et al., 2004). Although combustion itself is not considered in this analysis, combustion field is considered as the spatially distributed non-homogeneous temperature fields. Accordingly, the quantitative data on acoustic characteristics can be obtained and compared with the experimental data. Based on the numerical results, pressure oscillation in the combustor is diagnosed and the acoustic-damping effects of the present acoustic resonators, which are installed for combustion stabilization (Harrje and Reardon, 1972 ; NASA, 1974), are investigated extensively for its improved design.

2. Numerical Methods and Models

2.1 Numerical methods

The acoustic field in the combustion chamber is calculated through linear acoustic analysis and it is obtained by solving the following wave equation

$$\frac{1}{c^2}\frac{\partial^2 p}{\partial t^2}-\nabla^2 p=0, \tag{1}$$

where p is the pressure fluctuation caused by acoustic-wave propagation, t is the time, c is the sound speed, and ∇^2 is the Laplacian operator. The derivation of Eq. (1), the introduced approximations, and its boundary conditions are described in detail in the reference (Zucrow and Hoffman, 1977).

With a simple geometry of the chamber, the solution of Eq. (1) can be obtained analytically (Zucrow and Hoffman, 1977). In addition, the resonant frequency of each acoustic mode can be calculated analytically. For example, in a cylindrical chamber, each resonant frequency is expressed in the form,

$$f_{m,n,q}=\frac{c}{2}\left[\left(\frac{\alpha_{mn}}{R}\right)^2+\left(\frac{q}{L}\right)^2\right]^{1/2}, \tag{2}$$

where three indices of m, n, q denote the indices for tangential, radial, and longitudinal modes, respectively, α_{mn}'s eigenvalues-roots of the first spatial derivative of the Bessel function of the first kind, of order n, J_n, and R, L chamber radius and axial length, respectively. Since the gas turbine combustor is not cylindrical, Eq. (2) can not give the exact values of resonant frequencies. Nevertheless, the equation is useful to predict resonant frequencies in the right order of magnitude.

With a complex geometry of the chamber, the wave equation can be solved effectively by the finite element method (FEM) and the Galerkin method, which is one of FEMs, is used here (Chapra and Canale, 1989 ; SAS, 1993). Details on the solution procedures and principles based on the Galerkin method can be found in the literature (SAS, 1993). As a solver of the wave equation, the ANSYS code is adopted in this

study, which has been validated for acoustic analysis (Kang and Yoon, 1994; SAS, 1992).

2.2 Models

The selected combustion chamber is GT11N2 Silo combustor (Aigner and Müller, 1993; Lefebvre, 1998). Its geometry, dimension, and the computational grids are shown in Figs. 1 and 2. As shown in Fig. 2c, this combustor is equipped with the acoustic resonator, which is one of the combustion stabilization devices.

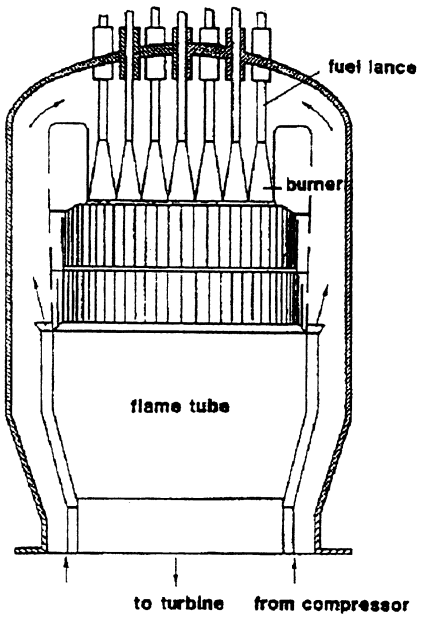

Fig. 1 Schematic diagram of the GT11N2 Silo combustor

The gas turbine combustor is connected with compressor and turbine, and working fluid flows continuously into and out of the combustor which is an open system. But, the inlet and the outlet of the combustor is relatively narrow and thus, wall boundary condition can be applied at all of outer boundaries surrounding the fluid. The fluid in the chamber is air of which the density is 1.21kg/m^3 and its speed of sound is 340m/s for cold-flow condition at 15.5℃. But, for hot-flow condition under which the combustion occurs, the temperature field is spatially non-homogeneous in the combustor and the non-homogeneity should be considered in order to evaluate the acoustic characteristics quantitatively. In this combustor, methane and air are adopted as fuel and oxidizer, respectively. Usually, lean methane-air flame is established in the combustor and it is assumed that there are only four species of CO_2, H_2O, O_2, and N_2 as the combustion products. With this assumption, the sound speed in the combustor can be calculated from the specific temperature.

In Fig. 3, the magnified acoustic resonators are shown and they consist of eleven short and six long resonators. In analyzing the acoustic field, about 23,000 to 30,000 elements are used for numerical calculation. This number of elements has been found to be enough to simulate acoustic behavior accurately in the present combustor.

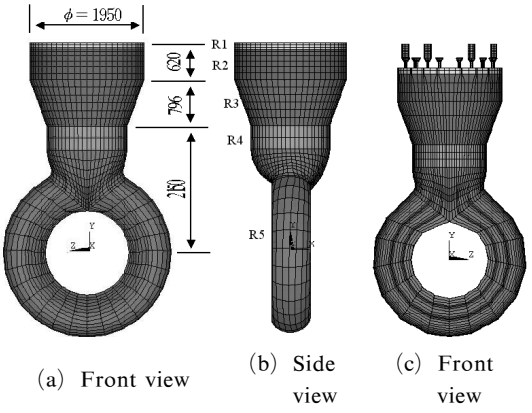

Fig. 2 Geometries and computational grids of combustors without/with acoustic resonators (R# indicates the region number).

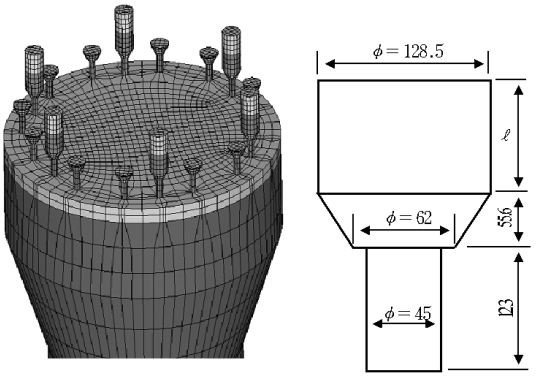

Fig. 3 Geometry and dimensions of the acoustic resonators (l=11.4 and 261.4mm for short and long resonators, respectively).

2.3 Numerical strategy

For the diagnosis of pressure oscillation in the combustor, first, the acoustic characteristics of the basic chamber-chamber without acoustic resonators installed- are investigated through a harmonic analysis (Sohn et al., 2004). The acoustic characteristics are identified by two factors, i.e., the natural or resonant frequencies and the acoustic damping factor of each acoustic mode. In the harmonic analysis, sound source is positioned on small area near the combustor wall, where the sinusoidal sine wave with the specific frequency is generated numerically as a function of time, and the resultant pattern of acoustic oscillation is calculated. And thereby, the natural acoustic modes, *i.e.*, first (1T), second (2T), and higher tangential modes (3T, ···), radial modes (1R, 2R, ···), longitudinal modes (1L, 2L, ···), and combined modes (1L1T, 1T1R, ···), are identified, and acoustic-pressure responses to the artificial acoustic excitation and damping factors are calculated. The sweeping frequency of acoustic excitation from the sound source with the amplitude of 10 Pa ranges from 50 to 600 Hz for cold condition and from 50 to 1, 100 Hz for hot condition, respectively. These ranges have approximately been predicted by Eq. (2) so that the resonant frequencies of the chamber fall in these frequency ranges. For hot condition, the approximate temperature distribution (Sattelmayer et al., 1992) is listed in Table 1. The monitoring point is near the combustor wall at the opposite side to the sound source on the identical cross-section, where the pressure amplitude is monitored.

The acoustic damping of each mode is quantified by a damping factor, η, which is defined from the bandwidth method (Laudien et al., 1995) as

$$\eta=\frac{f_2-f_1}{f_{peak}}, \tag{3}$$

where f_{peak} is the frequency at which the peak response (p_{peak}) is calculated, f_1 and f_2 are the frequencies at which the pressure amplitude corresponds to $p_{peak}/\sqrt{2}$ ($f_2>f_1$). This equation indicates that the damping factor becomes higher as the bandwidth normalized by the peak frequency, f_{peak}, is broadened on the plane of excitation frequency vs. acoustic-pressure response.

Next, the effects of acoustic resonators on the acoustic damping are investigated adopting the resonator-chamber - chamber with acoustic resonators installed. Acoustic resonators have the capacity to damp out the specific pressure oscillation with the same frequency as the tuning frequency of the resonator (Laudien et al., 1995). In the case of a Helmholtz-type resonator, the tuning frequency of acoustic resonator is written in the form (Laudien et al., 1995 ; Sohn and Kim, 2002),

$$f_0=\frac{c_{AC}}{2\pi}\sqrt{\frac{S}{V(l+\Delta l)}}, \tag{4}$$

where c_{AC} denotes the sound speed of fluid in the resonator, S cross-sectional area of the orifice connecting the resonator with the chamber, V the volume of the resonator, l the length of the orifice, and Δl is the mass correction factor, which is given approximately by 0.85 times the orifice diameter. To adjust the tuning frequency, f_0, the parameters of c_{AC}, S, V, l, and Δl can be varied in combination with each other based on Eq. (4). The present resonators shown in Fig. 3 have been designed based on this theoretical equation. But, when the geometry of the resonator is complex and deviates from that of the Helmholtz-type resonator, Eq. (4) may not give the exact tuning frequency. Accordingly, the present numerical analysis can give more accurate information on the actual tuning frequency of the resonators shown in Fig. 3. The acoustic effects of the resonators are identified by two factors, *i.e.*, the shift of natural or resonant frequencies and the increase in acoustic damping factor of the acoustic mode.

Table 1 Spatial temperature distribution in the combustor.

Region No.(Fluid Type)	Temperature [K]	Sound Velocity [m/s]
R1 (air)	653	512.3
R2 (combustion products)	1873	812.6
R3 (combustion products)	1673	768.0
R4 (combustion products)	1473	720.6
R5 (combustion products)	1277	670.9

3. Results and Discussions

3.1 Harmonic analysis of basic chamber for homogeneous cold condition

Acoustic responses to the pressure oscillation with the excitation frequency of 50 to 600Hz in the basic chamber are calculated for homogeneous cold condition (c=340m/s) and shown in Fig. 4. The increment of the frequency is 1.0 to 5.0Hz. There are found a number of peaks, which indicates thet each corresponding acoustic modes can be triggered into acoustic instability when the specific pressure oscillation is coupled in phase with heat-release-rate oscillation from combustion. Figure 5 demonstrates the acoustic fields resonated at the major low-order modes -2L, 1T, 2T, and 1R, where clear resonant acoustic fields are shown. As a result, it is found that the resonant frequencies of four modes are 65, 110, 175, and 225Hz, respectively. It is to be noted that in case of low-order transverse modes, *i.e.*, the 1st or 2nd tangential and radial modes, only the geometry of the flame tube dominates the resonant modes and their frequencies. The lower torus part of the combustor affects little the transverse modes.

From Fig. 4, in the basic chamber, the amplitudes of 1T and 2T are much higher than the other amplitudes and the absolute values of their amplitudes are over 60 Pa, which is so high compared with the amplitude of the imposed pressure wave, 10 Pa. This indicates that the chamber adopted here may be the most sensitive to acoustic oscillations of low-order tangential modes.

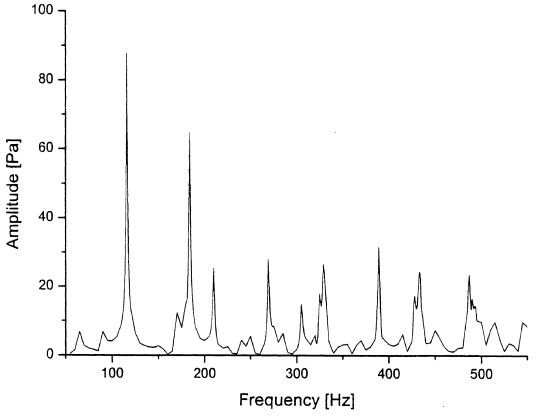

Fig. 4 Acoustic pressure responses of the basic chamber for homogeneous cold condition (c=340m/s).

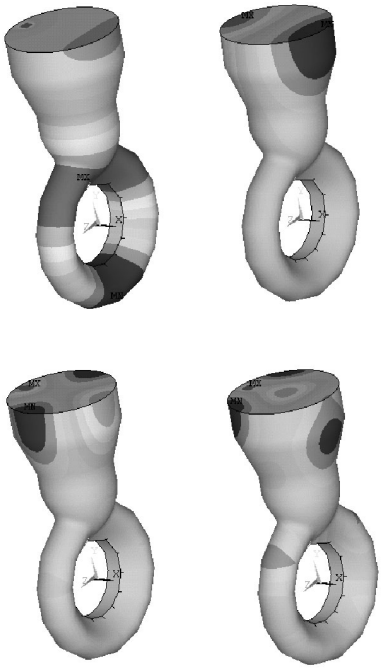

Fig. 5 Acoustic fields at several resonant frequencies (2L, 1T, 2T, and 1R) for homogeneous cold condition.

3.2 Harmonic analysis of basic chamber for non-homogeneous hot condition

Acoustic responses to the pressure oscillation with the excitation frequency of 50 to 1,100Hz in the basic chamber are calculated for non-homogeneous hot condition, under which temperature fields are distributed spatially as listed in Table 1, and they are shown in Fig. 6(a). The frequencies of the dominant peaks are 60, 256, 389, 435, 509, 627Hz, etc. It is worthy of note that the most dominant peak occurs at the frequency of 389 Hz, which has been found to be the 2nd tangential mode judging from the acoustic field. This is in contrast to the results for homogeneous cold condition in Fig. 4. Compared with the results for cold condition, the frequency values are increased

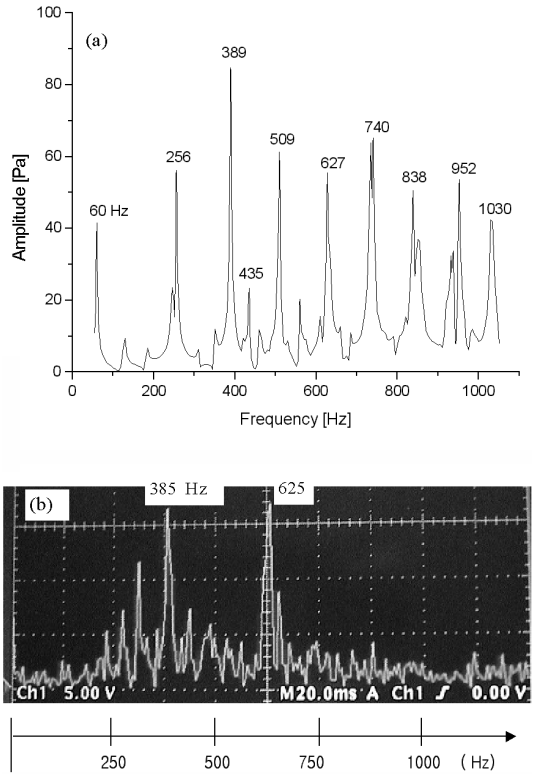

Fig. 6 Peak frequencies (a) acoustic pressure responses of the basic chamber for non-homogeneous hot condition, (b) measured frequencies of pressure oscillations during unstable combustion in high-power generation.

by factor of 2.2~2.3 due to higher fluid temperature, *i.e.*, higher sound speed in the chamber.

These peaks shown in Fig. 6(a) are compared with the experimental data shown in Fig. 6(b) in a quantitative manner. The measured frequencies of two most dominant peaks are 385 and 625Hz, which are almost the same values as the numerical data of 389 and 627Hz. Accordingly, it is probable that the pressure oscillation in the adopted chamber results from the acoustic instability and the reactive flow field in the flame tube excluding the torus part is mainly triggering the instability.

3.3 Tuning characteristics of acoustic resonators

The adopted resonators shown in Fig. 3 do not have the geometry of the Helmholtz-type resonator itself. Thus, it is not sure whether Eq. (4) can give the exact tuning frequency or not. This point can be verified through the harmonic analysis, of which the results for homogeneous cold condition are shown in Fig. 7. In this figure, the frequency at which the peak shows up is the tuning frequency of the acoustic resonator and thus, the tuning frequencies of long and short resonators are 85 and 201Hz, respectively. They are comparable with the values of 87 and 227Hz, respectively, which are calculated by Eq. (4), but with non-negligible error in case of short resonator.

In the case of a long resonator, the single peak shows up clearly, while the short resonator shows a number of non-negligible peaks near the one most dominant peak. On the other hand, the peak

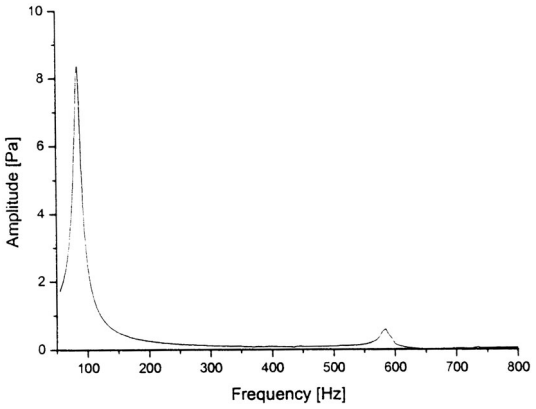

(a) Ratio of long-resonator response to chamber response

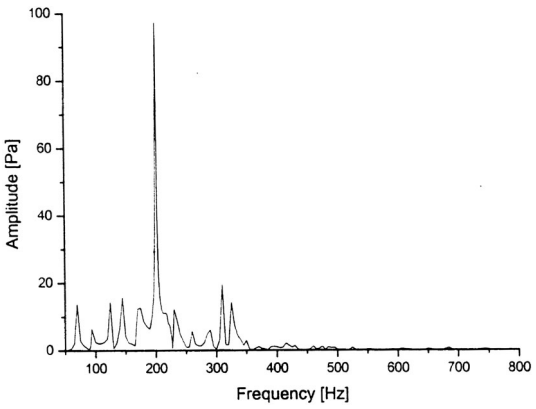

(b) Ratio of short-resonator response to chamber response

Fig. 7 Tuning characteristics of acoustic resonators for homogeneous cold condition.

amplitude from the long-resonator response is about 8 times larger than that from the chamber response, while that from the short-resonator response is nearly 100 times larger. Accordingly, the long resonator has a well-definable tuning frequency with relatively lower damping capacity and the short resonator has the ambiguous tuning frequency with higher damping capacity. In this study, the frequency of the most dominant peak is defined as the tuning frequency in case of short resonator.

The resonator volume of long resonator is 2.6 times larger than that of short resonator, and according to Eq. (4), the tuning frequency of short resonator should be 2.6 times larger than that of long resonator. But, it is not here, which indicates the tuning characteristics of short resonator deviates away from those predicted theoretically to a certain degree. This may be caused by an extremely small volume of the cylindrical part of short resonator as shown in Fig. 3.

3.4 Harmonic analysis of resonator-chamber for non-homogeneous hot condition

Acoustic responses to the pressure oscillation with the excitation frequency of 50 to 1,100 Hz in the resonator-chamber are calculated for non-homogeneous hot condition, and they are shown in Fig. 8. The resonators are filled with air at 380℃ (c=512.3m/s). From this figure, it is found that the long and short resonators are tuned to 127 and 301Hz, respectively, and the general pattern of the peaks is the same as that shown in Fig. 6(a).

The frequency shift caused by the resonator installation and the damping factors of the major peaks are summarized in Table 2, compared with the results from the basic chamber. As the effects of resonator installation, the resonant frequencies of several modes shift, but not so appreciably, and the damping factors are increased appreciably, especially at the resonant mode of which the frequency is close to the tuning frequency. Since the long cylinder is tuned close to the 2nd longitudinal mode of 128Hz, the specific mode has been damped out appreciably as shown in Fig. 9. But, it is found that the short cylinder is

Table 2 Damping factors of the major acoustic modes in the basic and resonator-chambers.

Frequency [Hz]		Damping Factor [%]	
Basic chamber	Resonator-chamber	Basic chamber	Resonator-chamber
60 (1L)	60	5.078	5.585 (10% ↑)
128 (2L)	131	2.648	7.027 (165% ↑)
256 (1T)	248	1.311	1.653 (26% ↑)
389 (2T)	394	1.012	1.326 (31% ↑)
509	510	0.813	0.857 (5.4% ↑)
627	627	0.812	1.305 (61% ↑)

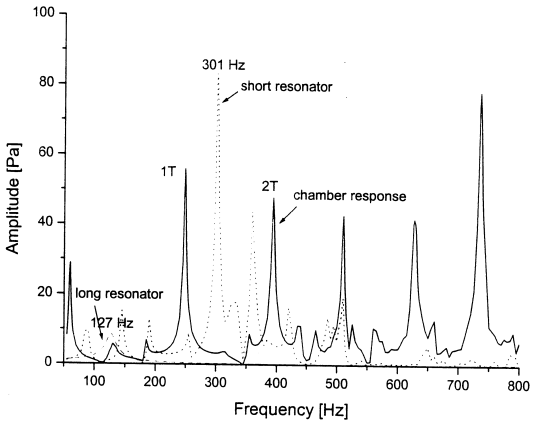

Fig. 8 Acoustic pressure responses of the resonator-chamber and resonators for non-homogeneous condition.

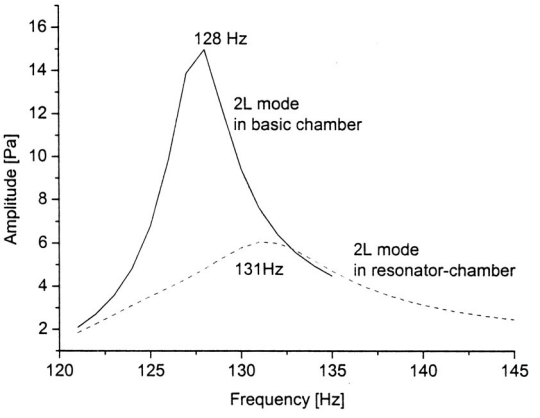

Fig. 9 Acoustic pressure responses of the combustion chamber, the 2nd longitudinal modes in the basic and resonator-chambers.

not tuned to any resonant modes and thereby, its damping effect is not appreciable. Accordingly, for the improvement of acoustic-damping effect, modification of eleven short resonators is required in view of their fine tuning. Furthermore, the long resonator needs to be tuned to the frequencies of dominant peaks at 1T and 2T modes rather than at 2L mode.

4. Concluding Remarks

The acoustic characteristics in the gas combustion combustor encountering with undesirable pressure oscillation have been investigated numerically through a linear acoustic analysis as a first step to analyze such pressure oscillation. Considering the spatial non-homogeneity of temperature field, the quantitative data on the harmful frequencies are obtained, which are in good agreement with the experimental data. This indicates that the pressure oscillation in the present combustor could result from acoustic instability.

The installation of the resonators with two different lengths, has appreciable effects on combustion stabilization when the resonator is tuned finely to the specific frequency to be damped out. But, the short resonator is not so finely tuned and modification is needed for enhancement of damping effects.

In the future work, optimization of acoustic resonators will be conducted in views of both fine tuning and higher damping capacity. Acoustic instability in the combustor will be simulated numerically considering the coupling between the combustion and the acoustics. Finally, the remedy for acoustic instability, i.e., the method to suppress the pressure oscillation, will be suggested and verified.

References

Aigner, M. and Müller, G., 1993, "Second-Generation Low-Emission Combustors for ABB Gas Turbines: Field Measurements with GT11N-EV," *Journal of Engineering for Gas Turbines and Power*, Vol. 115, pp. 533~536.

Chapra, S. C. and Canale, R. P., 1989, *Numerical Methods for Engineers*, 2nd ed., McGraw-Hill, Singapore.

Culick, F. E. C. and Yang, V., 1995, in *Liquid Rocket Engine Combustion Instability* (V. Yang, and W. E. Anderson, eds.), *Progress in Astronautics and Aeronautics*, Vol. 169, AIAA, Washington DC, pp. 3~38.

Fleifil, M., Annaswamy, A. M., Ghoniem, Z. A., and Ghoniem, A. F., 1996, "Response of a Laminar Premixed Flame to Flow Oscillations: A Kinematic Model and Thermoacoustic Instability Results," *Combustion and Flame*, Vol. 106, pp. 487~510.

Harrje, D. J. and Reardon, F. H. (eds.), 1972, *Liquid Propellant Rocket Combustion Instability*, NASA SP-194.

Kang, K. T. and Yoon, J. K., 1994, "Analysis of Combustion Instability in a Smokeless Propellant Rocket Motor," *Transactions of The KSME (B)*, Vol. 18, No. 11, pp. 3032~3038.

Laudien, E., Pongratz, R., Pierro, R., and Preclik, D., 1995, in *Liquid Rocket Engine Combustion Instability* (V. Yang, and W. E. Anderson, eds.), *Progress in Astronautics and Aeronautics*, Vol. 169, AIAA, Washington DC, pp. 377~399.

Lefebvre, A. H., 1998, *Gas Turbine Combustion*, 2nd ed., Taylor & Francis, Ann Arbor, MI.

McManus, K. R., Poinsot, T., and Candel, S. M., 1993, "A Review of Active Control of Combustion Instabilities," *Progress in Energy and Combustion Science*, Vol. 19, pp. 1~29.

NASA, 1974, "Liquid Rocket Engine Combustion Stabilization Devices," NASA SP-8113.

SAS, 1992, *ANSYS User's Manual for revision 5.0*, Volume I, Procedures, Swanson Analysis Systems, Inc., Houston, PA.

SAS, 1993, *ANSYS User's Manual for revision 5.0*, Volume IV, Theory, Swanson Analysis Systems, Inc., Houston, PA.

Sattelmayer, T., Felchlin, M. P., Haumann, J., Hellat, J., and Styner, D., 1992, "Second-Generation Low-Emission Combustors for ABB Gas Turbines: Field Measurements with GT11N-EV," *Journal of Engineering for Gas Turbines and Power*, Vol. 114, pp. 118~125.

Seo, S., 2003, "Combustion Instability Mechanism of a Lean Premixed Gas Turbine Combustor," *KSME International Journal*, Vol. 17, No. 6, pp. 906～913.

Sohn, C. H., 2002a, "Unsteady Analysis of Acoustic Pressure Response in N_2 Diluted H_2 and Air Diffusion Flames," *Combustion and Flame*, Vol. 128, pp. 111-120.

Sohn, C. H., 2002b, "A Numerical Study on Acoustic Behavior in Baffled Combustion Chambers," *Transactions of the KSME(B)*, Vol. 27, No. 1, pp. 966～975.

Sohn, C. H., Chung, S. H., Kim, J. S., and Williams, F. A., 1996, "Acoustic Response of Droplet Flames to Pressure Oscillations," *AIAA Journal*, Vol. 34, No. 9, pp. 1847-1854.

Sohn, C. H., Kim, S.-K., and Kim, Y.-M., 2004, "Effects of Various Baffle Designs on Acoustic Characteristics in Combustion Chamber of Liquid Rocket Engine," *KSME International Journal*, Vol. 18, No. 1, pp. 154～161.

Sohn, C. H. and Kim, Y.-M., 2002, "A Numerical Study on Acoustic Behavior in Combustion Chamber with Acoustic Cavity," *Journal of The Korean Society for Aeronautical and Space Sciences*, Vol. 30, No. 4, pp. 28～37.

Wicker, J. M., Yoon, M. W., and Yang, V., 1995, "Linear and Non-linear Pressure Oscillations in Baffled Combustion Chambers," *Journal of Sound and Vibration*, Vol. 184, pp. 141～171.

Yang, Y. J., Akamatsu, F., and Katsuki, M., 2003, "Characteristics of Self-excited Combustion Oscillation and Combustion Control by Forced Pulsating Mixture Supply," *KSME International Journal*, Vol. 17, No. 11, pp. 1820～1831.

Zucrow, M. J. and Hoffman, J. D, 1977, *Gas Dynamics*, Vol. II, John Wiley & Sons, Inc., New York.